Support Vector Machine for Urban Land-use Classification using Lidar Point Clouds and Aerial Imagery

Haiyan Guan*[a], Jonathan Li[a] , Michael A. Chapman[b], Liang Zhong[c], Que Ren[a]
[a]Dept. Geography and Environmental Management, University of Waterloo,
200 University Ave. West, Waterloo, ON, Canada N2l 3G1
[b]Dept. Civil Engineering, Ryerson University,
350 Victoria Street, Toronto, ON, Canada M5B 2K3
[c]School of Remote Sensing and Information Engineering, Wuhan University,
129 Luoyu Road, Wuhan, Hubei, China

ABSTRACT

Support Vector Machine (SVM), as a powerful statistical learning method, , has been found that its performance on land-use -classification outperform conventional classifiers using multiple features extracted from lidar data and imagery. Therefore, in this paper, we use SVM for urban land-use classification. First, we extract features from lidar data, including multi-return, height texture, intensity; other spectral features can be obtained from imagery, such as red, blue and green bands. Finally, SVM is used to automatically classify buildings, trees, roads and ground from aerial images and lidar point clouds. To meet the objectives, the classified data are compared against reference data that were generated manually and the overall accuracy is calculated. We evaluated the performance of SVMs by comparing with classification results using only lidar data, which shows that the land use classification accuracy was improved considerably by fusing lidar data with multispectral images. Meanwhile, comparative experiments show that the SVM is better than Maximum Likelihood Classifier in urban land-use classification.

Keywords: SVM, Land use, Classification, Features, Lidar, Imagery

1. INTRODUCTION

Land-use classification has always been an active research topic in remote sensing community. Today, most airborne light detection and ranging (lidar) systems can collect point cloud data and image data simultaneously. Higher land-use classification accuracy of complex urban areas becomes achievable when both types of data are used. An airborne lidar system can directly collect a digital surface model (DSM) of an urban area. Unlike a digital terrain model (DTM), the DSM is a geometric description of both terrain surface and objects located on and above this surface like buildings and trees. Lidar-derived dense DSMs have been shown to be useful in building detection, which is a classification task that separates buildings from other objects such as natural and man-made surfaces (lawn, roads) and vegetation (trees).

Traditional aerial imagery can provide an abundant amount of structure, intensity, colors, and texture information. However, it is difficult to recognize objects from aerial imagery due to image interpretation complexity. Thus, the complementary informational content of lidar point clouds and aerial imagery contribute to urban object classification. The development of lidar system, especially incorporated with high-resolution camera component, and limitations of lidar data urged researchers to fuse imagery into lidar data for land-use classification (Haala et al., 1998; Zeng et al., 2002; Rottensteiner et al., 2003; Collins et al., 2004; Hu and Tao, 2005; Walter, 2005; Rottensteiner et al., 2005; Brattberg and Tolt, 2008; Chehata et al., 2009; Awrangjeb et al., 2010). Besides multispectral imagery, (Haala and Brenner, 1999; Bartels and Wei, 2006) used color infrared (CIR) imagery to perform a pixel-based land-use classification.

* h6guan@uwaterloo.ca, phone 1 519 616-6026

Haala and Walter (1999) integrated the height information an additional channel, together with the spectral channels into a pixel-based classification scheme. Charaniya et al. (2004) described a supervised classification technique that classify lidar data into four classes-road, meadow, building and tree-by combining height texture, multi-return information and spectral feature of aerial images. Brennan and Webster (2006) presented a rule-based object-oriented classification approach to classifying surfaces derived from DSM, intensity, multiple returns, and normalized height (Tiede et al. 2008). Germaine and Hung (2010) proposed two-step classification methodology to delineate impervious surface in an urban area using lidar data to refine a base classification result of multispectral imagery based on ISODATA. Their experiment showed that the use of lidar data can improve the overall accuracy by 3%. Therefore, the implementation of lidar significantly enhances the classification of optical imagery both in terms of accuracy as well as automation. Rottensteiner et al. (2007) demonstrated that the classification accuracy of a small residential area can be improved by 20% when fusing airborne lidar point cloud with multispectral imagery. Huang et al. (2008) showed that the performance of urban classification by integrating lidar data and imagery are better than other classification methods only using single data source.

The Support Vector Machine (SVM), based on statistical learning theory, has been found that its performance on land-use classification outperform traditional or conventional classifier (Yang, 2011), and has become a first choice algorithm for many remote sense users. Being a non-parametric classifier SVM is particularly suitable for classifying remotely sensed data of high dimensionality and from multiple sources (Lodha, 2006; Waske and Benediktsson, 2007; Malpica, 2010). Classification procedures based on the SVM have been applied to multispectral, hyperspectral data, synthetic aperture radar (SAR) data, and lidar data. Therefore, in the project, the SVM classifier is suited to classifying objects by using multiple features extracted from lidar data and imagery.

This paper is organized as follows. In Section 2, we describe the basic principles of SVM for classification, the lidar data and calibrated imagery used in the paper, features selected from the lidar data and imagery, respectively. Section 3 then discusses the SVM classification results using only lidar data comparing with integration of lidar data and image data, and compares results of SVM by Maximum Likelihood Classifier (MLC). Finally Section 4 concludes the proposed method.

2. METHODOLOGY

2.1 Principles of SVM

SVM, introduced in 1992 (Boser et al, 1992), have recently been used in numerous applications in the field of remote sensing. Mountrakis (2011) indicated that SVMs are particularly appealing in the remote sensing field due to their ability to generalize well even with limited training samples, a common limitation for remote sensing applications. SVMs are typically a supervised classifier, which requires training samples. Literature shows that SVMs are not relatively sensitive to training sample size and have been improved to successfully perform with limited quantity and quality of training samples. Dalponte et al. (2008) point out that SVMs outperformed Gaussian maximum likelihood classification and k-NN technique (Angelo et al, 2010), and that the incorporation of lidar variables generally improved the classification performance. In this section we will briefly describe the basic SVMs concepts for classification problems.

The main advantage of SVMs is given by the fact that it can find an optimal hyper-plane learnt from the spatial distribution of training data in the feature space. SVM aims to discriminate two classes by fitting an optimal separating hyper-plane to the training data within a multi-dimensional feature space *Z*, by using only the closest training samples (Melgani, 2004)Thus, the approach only considers samples close to the class boundary and works well with small training sets, even when high dimensional data sets are classified.

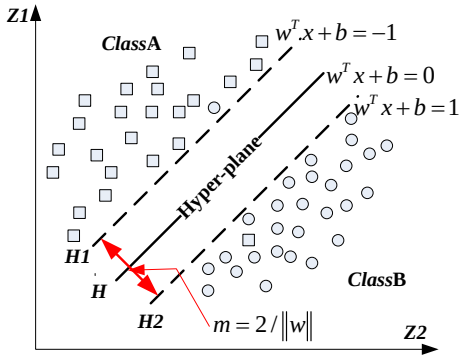

Fig. 1 an optimum separating hyper-plane

Figure 1 demonstrates the basic concepts of the SVM classification, in which *m* is the distance between *H1* and *H2*, and *H* is the optimum separating hyper-plane which is defined as:

$$wx+b=0 \tag{1}$$

where *x* is a point on the hyper-plane, *w* is an n-dimensional vector perpendicular to the hyper-plane, and *b* is the distance of the closet point on the hyper-plane to the origin. It can be shown that:

$$wx+b\le -1,\rightarrow \quad class\mathrm{A} \tag{2}$$

$$wx+b\ge 1,\rightarrow \quad class\mathrm{B} \tag{3}$$

Equations (2) and (3) can be combined into:

$$\mathrm{y}_i\left[wx_i+b\right]-1\ge 0 \qquad \forall i \tag{4}$$

The SVM attempts to find a hyper-plane, Equation (1), with minimum $w^T w$ that is subject to constraint (4). The classification processing to find the optimum hyper-plane is equivalent to solving quadratic programming problems:

$$\begin{aligned} &\min \quad \frac{1}{2}w^T w+C\sum_{i=1}^{l}\xi_i \\ &S.t\begin{cases} y_i\left[w^T\phi(x_i)+b\right]\ge 1-\xi_i \\ \xi_i\ge 0, \quad i=1,2,\cdots\cdots,l \end{cases} \end{aligned} \tag{5}$$

where C is the penalty parameter which controls the edge balance of the error ξ using the technique of Lanrange multipliers, the optimization problem becomes:

$$\begin{aligned} &\min \quad \frac{1}{2}\sum_{i=1}^{l}\sum_{j=1}^{l}\alpha_i\alpha_j y_i y_j K(x_i y_j)-\sum_{i=1}^{l}\alpha_i \\ &S.t \quad \begin{cases} \sum_{i=1}^{l} y_i\alpha_i=0 \\ 0\le\alpha_i\le C, \quad i=1,2,\cdots\cdots,l \end{cases} \end{aligned} \tag{6}$$

where $K(x_i y_j)=\phi(x_i),\phi(y_j)$ is kernel function, the functions used to project the data from input space into feature space. The kernel function implicitly defines the structure of the high dimensional feature space where a maximal margin hyper-plane will be found. A feature space would cause the system to overfit the data if it includes too many features, and conversely the system might not be capable of separating the data if the kernels are too poor. Four kernel functions are available namely: Gaussian radial basis function (RBF), see Equation (7), linear, polynomial and sigmoid. We chose the Gaussian RBF kernel for our SVM classifiers, since RBF kernels have yielded extremely high accuracy rates for the

most challenging high-dimensional image classifications, such as those involving hyper-spectral imagery or a combination of hyper-spectral imagery and lidar data (Melgani, 2004).

$$K(x_i, y_j) = e^{(-\frac{1}{2\delta}\|x_i - y_j\|^2)} \tag{7}$$

SVM by itself is a binary. LULC applications usually needs to divide the data set into more than two classes. In order to solve for the binary classification problem that exists with the SVM and to handle the multi-class problems in remotely sensed data, two popular approaches are commonly used. One-Against-One is the method that calculates each possible pair of classes of a binary classifier. Each classifier is trained on a subset of training examples of the two involved classes. All *N (N-1)/2* binary classifications are combined to estimate the final output. When applied to a data set, each classification gives one vote to the winning class and the point is labelled with the class having most votes. This approach is suitable for problem with large amount of data. One-Against-All involves training a set of binary classifiers to individually separate each class from the rest. Anthony et al. (2007) have reported that the resulting classification accuracy from One-Against-All method is not significantly different from One-Against-One approach and the choice of technique adopted is based on personal preference and the nature of the used data. In the paper, we use the One-Against-All technique since the One-Against-One technique results in a larger number of binary SVMs and need intensive computations, but also the One-Against-All method, for an N-class problem, constructs N SVM models, which is trained to tell the samples of one class from samples of all remaining classes.

2.2 Data Description

Figure 2 shows the study dataset, which was collected over 1,000 m above ground level by Optech ALTM 3100 system. The data sets covered a residential area of 981 m × 819 m in the City of Toronto, Ontario, Canada.The lidar dataset consists of the first- and last- returns of the laser beam. The true color image data used were taken by an onboard 4k × 4k digital camera simultaneously.

Figure 2 (a) shows a raster DSMs, containing a total of 803,439 points, which were interpolated with the first and the last pulse return by the bi-linear interpolation method. The width and height of the grid equals to the ground sample distance (GSD) of the aerial image (0.5 m). The elevation of the study area ranges from 148.71 m to 178.11 m. Besides buildings, several clusters of trees located along the street; (b) demonstrates the intensity image of lidar data with the same resolution as the DSM; (c) shows a true color aerial image that was re-sampled to 0.5 m ground pixel. The majority of buildings appeared in the color image are with gable roofs or hip roofs.

(a) (b) (c)

Fig. 2 Data sets: (a) DSM of lidar data; (b) intensity image of lidar data; (c) aerial orthophoto

2.3 Feature Selection

We use the SVM algorithm to classify the data set into four classes (trees, buildings, grass and roads). Since the SVM requires a feature vector for each lidar point to be classified, there are six features selected from lidar data and aerial imagery for urban land-use classification, including multi-return information, height texture, lidar intensity and three image bands **(RED, BLUE and GREEN)**. Feature selection is very crucial as meaningful features facilitate classification accuracy of the data set.

- **Feature 1: Lidar Multi-return Information (LHr):** Height information between first- and last- returns usually differentiates tree features from lidar data. One of lidar system's characteristics is the capability of laser beam to

penetrate the trees canopy through a small opening. The number of returns counts on the object within the travel path of the laser pulse. Many commercial lidar systems can measure multiple returns.

- **Feature 2: Lidar height texture (LHt):** A range image, different from traditional optic images, is based on the raw lidar point clouds and created by interpolation. Every pixel in range image represents a certain height value. The brighter a pixel is, the higher its height is. In other words, the value of a pixel is proportional to its height value. (Mass, 1999) points out height texture defined by local height variations is a significant feature of objects to be recognized. By applying image processing algorithms the gradient magnitude image of the range image can be calculated, containing information about height variations, which is useful in differentiation of man-made objects and natural objects.
- **Feature 3: Lidar intensity (Li):** The intensity is related to the reflective properties of the targets as well as the light used, and different material has different reflectance. Similar to low-resolution aerial images, lidar intensity information can be used to extract planimetric features and serve as ancillary input for lidar data processing.
- **Features 4 to 6: Three image bands (R, B and G) from the aerial image:** The spectral information of aerial image correspond to the response of all objects on terrain surface to visible light.

Thus, the resulting of feature vector for each lidar point is given by $Fv = \begin{bmatrix} LHr & LHt & Li & R & G & B \end{bmatrix}^T$. All feature values were normalized in the range of [-1, 1].

In this study, about 17,039 candidate points were randomly selected as training data sets, and about 15% points, or the total of 105,298 were used for validation. The Terrascan model of Terrasoild® was used to manually edit the training data sets.

3. RESULTS AND DISCUSSION

3.1 Experiments and Results

Two parameters should be specified while using the RBF kernels: C and the kernel function γ. The problem is that there is no rule for the selection of the kernel's parameters and it is not known beforehand which C and γ are the best for the current problem (Lin and Lin, 2003). Both parameters C and γ depend on the data range and distribution and they differ from one classification problem to another (Van der Linden et al., 2009). In the paper, we select these parameters empirically by trying a finite number of values and keeping those that provide the least test error. The results of optimization for C and γ are 300, and 0.4, respectively.

Fig. 3(a) shows the results of SVM using lidar data and aerial image data. Four classes-buildings, grass, tress and roads are separated from each other very well. There are some classification error occurred around some building boundaries, which are misclassified as trees because of the selected multi-return feature. Although the laser beam can penetrate the trees canopy to the ground, the height information between first- and last-return is unreliable to distinguish the tree from the lidar point clouds. This is because the laser beam hitting on the edge of building also generates two returns. Secondly, if the density of trees is high, the small-footprint lidar cannot penetrate the tree's canopy.

(a) (b) (c)

Fig. 3 Classification sults obtained by (a) SVM using lidar data and aerial image, (b) SVM using lidar data, and (c) MLC using lidar data and aerial image.

3.2 Quantitative Assessment

To evaluate the overall performance of our classification method, we utilized software Terrasolid to produce the reference data for comparing with the classified results on a pixel-by-pixel basis. One of the most common methods of expressing classification accuracy is the preparation of a classification error matrix (confusion matrix). An error matrix is an effective way to assess accuracy in that it compares the relationship between known reference data and the corresponding results of the classification (Congalton, 1991). It is a square matrix E of $N \times N$ elements, where N is number of classes. The element E_{ij} is the number of points known to belong to class i and classified as belonging to class *j*. Thus, the elements on the leading diagonal E_{ii} correspond to correctly classified points, whereas the off-diagonal elements correspond to erroneous classifications (i.e., the commission and omission errors). From the confusion matrix, overall accuracy (OA) (Story and Congalton, 1986) can be calculated.

Table 1. Results of SVM classification

	Reference data				
SVMs Classification	Class	Buildings	Roads	Tree	Grass
	Buildings	22980	206	2317	37
	Roads	2219	32726	2384	3477
	Tree	1097	1394	14552	91
	Grass	63	3077	279	18431
OA= (22980+32726+14552+18431)/ 105298=84.23%					

Table 1 and Figure 3(a) show the classification obtained using the SVM algorithm. These results show that the proposed method produced 84.23% in overall classification accuracy.

Figure 3(b) shows the SVM classification results using lidar data alone. Intensity information of lidar data is utilized to separate grass from roads. However, there are severe "salt and pepper" phenomena, and some low buildings between high ones are misclassified as roads because of a lack of spectral information. And part of roads also misclassified as class grass due to their intensity information similar to characteristics reflected from grass. Finally, the overall accuracy is 81.78%. Therefore, integration of lidar point clouds and aerial images can improve the accuracy of classification.

3.3 Comparison with Maximum Likelihood Classifier

In this section, we compare results of proposed method by MLC, the classification results shown in the Figure 3(c). The visual inspection shows that MLC is not as robust as SVM because there, besides "salt and pepper" noise, are unexpectedly misclassified points comparing with the classification results obtained using the SVM method. More building boundary points are mistakenly labelled as tree points; buildings are confused with roads. Table 2 illustrates the error matrix of MLC. The overall accuracy of classification is 77.41%. Therefore, the comparison of the SVM method with the MLC method demonstrates that use of the SVM method can improve overall accuracy by about 7 % in the land-use classification process.

Table 2. Results of MLC classification

	Reference data				
MLC	Class	Buildings	Roads	Tree	Grass

	Buildings	20055	2207	4192	86
	Roads	3719	31101	2487	3499
	Tree	246	1927	12279	365
	Grass	214	2976	574	18086
OA=77.41%					

4. CONCLUSIONS

In this paper we have presented a classification method based on SVM using aerial imagery along with lidar point clouds, which classified the dataset into four classes: buildings, trees or high vegetation, grass and roads. The SVM classification method could solve sparse sampling, non-linear, high-dimensional data, and global optimum problems. In our proposed methodology, we have used One-Against-All SVMs with the RBF kernel because it can analysis higher-dimensional data and requires that only two parameters, C and γ. The fusion of multi-source data could obtain more accurate information than a single data source is used. Spectral information of aerial imagery integrated with lidar point clouds results in a significantly higher accuracy than using lidar range data alone. Compared with the MLC method, our results demonstrate that the SVM method can achieve higher overall accuracy in urban land-use classification.

REFERENCES

[1] Angelo, J. J., B. W. Duncan, and J, F. Weishampel, "Using lidar-derived vegetation profiles to predict time since fire in an oak scrub landscape in east-central Florida," *Remote Sensing*, 2010, 2, 514-525;

[2] Anthony, G., H. Gregg, and M. Tshilidzi, "Image Classification using SVMs: One-against-One Vs One-against-All," In: *Proc. 28th Asian Conference on Remote Sensing* Kuala Lumpur, Malaysia,12-16 November 2007.

[3] Awrangjeb, M., M. Ravanbakhsh and C.S. Fraser, "Automatic detection of residential buildings using lidar data and multispectral imagery," *ISPRS Journal of Photogrammetry and Remote Sensing*, 65(5), 457-467(2010).

[4] Bartels, M., and H. Wei, " Maximum likelihood classification of lidar data incorporating multiple co-registered bands," *Proceedings of 4th International Workshop on Pattern Recognition in Remote Sensing/18th International Conference on Pattern Recognition*, 20 August, Hong Kong, China, pp.17-20, (2006).

[5] Boser, B. E., I. M. Guyon, and V. N. Vapnik, "A training algorithm for optimal margin classifiers," *Proceedings of the 5th Annual ACM Workshop on Computational Learning Theory*, (1992), pp. 144-152 ,(1992).

[6] Brattberg, O. and G. Tolt, "Terrain classification using airborne lidar data and aerial imagery," *International Archives of the Photogrammetry, Remote Sensing and Spatial Information Sciences*, 37 (B3b): 261-266, (2008).

[7] Brennan, R. and T. L. Webster, "Object-oriented land cover classification of lidar derived surfaces," *Canadian Journal of Remote Sensing*, 32 (2): 162-172, (2006).

[8] Charaniya, A.P., R. Manduchi, M. Roberto and S.K. Lodha, "Supervised parametric classification of aerial lidar data," *Proceedings of the IEEE Conference on Computer Vision and Pattern Recognition Workshop*, 27 June - 2 July, Baltimore, MD. Vol. 3, pp. 25-32, (2004).

[9] Chehata, N., L. Guo and M. Clement, "Contribution of airborne full-waveform lidar and image data for urban scene classification," *Proceedings of the 16th IEEE International Conference on Image Processing*, 7-11 November, Cairo, Egypt, pp.1669-1672, (2009).

[10] Collins, C. A., R. C. Parker, and D.L. Evans, "Using multispectral imagery and multi-return lidar to estimate trees and stand attributes in a southern bottomland Hardwood forest," Proceedings of 2004 ASPRS Annual Conference, May 23-28, Denver, Colorado, unpaginated CD-ROM,(2004).

[11] Congalton, R.G., "A review of assessing the accuracy of classifications of remotely sensed data," *Remote Sensing of Environment*, 37(1): 35-46,(1991).

[12] Dalponte, M., L. Bruzzone, and D. Gianelle, "Fusion of hyperspectral and LIDAR remote sensing data for classification of complex forest areas," *IEEE Transactions on Geoscience and Remote Sensing*, 46 (5), 1416–1427,(2008).

[13] Germaine, K. A. and M. Huang, "Delineation of impervious surface from multispectral imagery and lidar incorporating knowledge based expert system rules," *Photgrammetric Engineering & Remote Sensing*, 77(1):77-87, (2011).

[14] Mountrakis, G., J. Im, C. Ogole, "Support vector machines in remote sensing: A review," *ISPRS Journal of Photogrammetry and Remote Sensing*, (2011).

[15] Haala, N. and V. Walter, "Automatic classification of urban environments for database revision using lidar and color aerial imagery," International Archives of Photogrammetry and Remote Sensing, 32(7-4-3W6): 76-82, (1999).

[16] Haala, N. and C. Brenner, "Extraction of buildings and trees in urban environments," *ISPRS Journal of Photogrammetry and Remote Sensing*, 54(2–3):130–137, (1999).

[17] Hu, Y. and C. V. Tao, "Hierarchical recovery of digital terrain models from single and multiple return lidar data," Photogrammetric Engineering & Remote Sensing, 71 (4): 425–433,(2005).

[18] Huang, M., S. Shyue, L. Lee, and C. Kao, "A knowledge-based approach to urban feature classification using aerial imagery with lidar data," *Photogrammetric Engineering & Remote Sensing*, 74(12):1473-1485, (2008).

[19] Lin, H.T. and C.-J. Lin. A study on sigmoid kernels for SVM and the training of non-PSD kernels by SMO-type methods. Technical report, Department of Computer Science, National Taiwan University, (2003).

[20] Lodha, S. K., E. J. Kreps, D. P. Helmbold, and D. Fitzpatrick, "Aerial lidar data classification using support vector machines (SVM)," *Proceedings of the Third International Symposium on 3D Data Processing, Visualization, and Transmission (3DPVT'06).*

[21] Malpica, J. A. and M. C. Alonso, "Urban changes with satellite imagery and lidar data," *International Archives of the Photogrammetry, Remote Sensing and Spatial Information Science,* 38(8), Kyoto Japan 2010.

[22] Mass, H.-G., "The potential of height texture measures for the segmentation of airborne laser scanner data," *Proceedings of 21st Canadian Symposium on Remote Sensing*, 21-24 June, Ottawa, Ontario, Canada, Vol. 1, pp.154-161, (1999).

[23] Melgani, F. and L. Bruzzone, "Classification of hyperspectral remote sensing images with support vector machines," *IEEE Transactions on Geoscience and Remote Sensing,* vol. 42, no. 8, pp. 1778–1790, Aug. 2004.

[24] Rottensteiner, F., J. Trinder, S. Clode and K. Kubik, "Detection of buildings and roof segments by combining lidar data and multispectral images," *Image and Vision Computing*, 26-28 November, Massey University, Palmerston North. New Zealand, pp. 60-65, (2003).

[25] Rottensteiner, F., J. Trinder, S. Clode and K. Kubik, "Using the Dempster–Shafer method for the fusion of lidar data and multispectral images for building detection," *Information Fusion*, 6(4): 283-300, (2005).

[26] Rottensteiner, F., J. Trinder, S. Clode and K. Kubik, "Building detection by fusion of airborne laser scanner data and multispectral images: Performance evaluation and sensitivity analysis," *ISPRS Journal of Photogrammetry and Remote Sensing*, 62(2):135-149, (2007).

[27] Story M. and R. G. Congalton, "Accuracy assessment: A user's perspective," *Photogrammetric Engineering & Remote Sensing*, 52 (3): 397–399, (1986).

[28] Tiede, D., S. Lang and C. Hoffmann, *Domain-specific class modeling for one-level representation of single trees, Object-Based Image Analysis*. Springer, New York, pp. 133-151, (2008).

[29] van der Linden, S., Udelhoven, T., Leitao, P., J., Rabe, A., Damm, A., Hostert, P., "SVM regression for hyperspectral image analysis". *6th Workshop EARSeL SIG Imaging Spectroscopy*. Tel Aviv, Israel, (2009).

[30] Walter, V., "Object-based classification of integrated multispectral and lidar data for change detection and quality control in urban areas," *Proceedings of URBAN 2005/ URS 200*5, 14-16 March, Tempe, AZ, unpaginated CD-ROM, (2005).

[31] Waske, B., and J. A. Benediktsson, "Fusion of support vector machine for classification of multisensory data," *IEEE Transactions on Geoscience and Remote Sensing*, 45(12): 3858-3866, (2007).

[32] Yang, X., "Parameterizing support vector machines for land cover classification," *Photogrammetric Engineering & Remote Sensing*, 77(1):27-37, (2011).

[33] Zeng, Y., J. Zhang, G. Wang and Z. Lin, "Urban land-use classification using integrated airborne laser scanning data and high resolution multispectral satellite imagery," *Proceedings of Pecora15/Land Satellite Information IV/ISPRS Commission I/FIEOS 2002 Conference*, 10-15 November, Denver, CO, unpaginated CD-ROM, (2002).